Bone material properties and response to teriparatide in osteoporosis due to WNT1 and PLS3 mutations

Fratzl-Zelman, Nadja

2021-05

Fratzl-Zelman , N , Wesseling-Perry , K , Mäkitie , R E , Blouin , S , Hartmann , M A , Zwerina , J , Valimaki , V-V , Laine , C M , Välimäki , M J , Pereira , R C & Mäkitie , O 2021 , ' Bone material properties and response to teriparatide in osteoporosis due to WNT1 and PLS3 mutations ' , Bone , vol. 146 , 115900 . https://doi.org/10.1016/j.bone.2021.115900

http://hdl.handle.net/10138/341317
https://doi.org/10.1016/j.bone.2021.115900

Bone material properties and response to teriparatide in osteoporosis due to *WNT1* and *PLS3* mutations

Nadja Fratzl-Zelman#[1], Katherine Wesseling-Perry#[2], Riikka E. Mäkitie[3], Stéphane Blouin[1], Markus A. Hartmann[1], Jochen Zwerina[1]; Ville-Valtteri Välimäki[4], Christine M. Laine[6,7], Matti J. Välimäki[8], Renata C. Pereira§[2], Outi Mäkitie§[3,6,9]

# The first and second authors contributed equally to this manuscript

§ The final and penultimate authors contributed equally to this manuscript

1. Ludwig Boltzmann Institute of Osteology at the Hanusch Hospital of OEGK and AUVA Trauma Centre Meidling, 1st Medical Department, Hanusch Hospital, Vienna, Austria

2. Department of Pediatrics, David Geffen School of Medicine at UCLA, Los Angeles, USA

3. Folkhälsan Institute of Genetics and University of Helsinki, Helsinki, Finland

4. Department of Orthopaedics and Traumatology, Helsinki University Central Hospital and Helsinki University, Jorvi Hospital, Espoo, Finland

5. Department of Orthopedics, Institute of Clinical Sciences, Sahlgrenska University Hospital and University of Gothenburg, Gothenburg, Sweden

6. Children's Hospital, University of Helsinki and Helsinki University Hospital, Helsinki, Finland,

7. Department of Endocrinology, Institute of Medicine, Sahlgrenska University Hospital and University of Gothenburg, Gothenburg, Sweden

8 Division of Endocrinology, Department of Medicine, Helsinki University Central Hospital, Helsinki, Finland

9 Department of Molecular Medicine and Surgery, Karolinska Institutet, and Department of Clinical Genetics, Karolinska University Hospital, Stockholm, Sweden

Abbreviated title: Matrix mineralization in *WNT1* and *PLS3* mutations

Keywords: quantitative backscattered electron microscopy, bone mineralization density distribution, teriparatide, histomorphometry, FGF23

Word Count: 3925

Number of figures and tables: 4 tables; 6 figures

Corresponding author/author to whom reprint requests should be addressed

Katherine Wesseling Perry

A2-383 MDCC

650 Charles Young Drive

Los Angeles, CA 90095

Phone: 310-206-6987

Fax: 310-825-0442

Email: kwesseling@mednet.ucla.edu

Financial support: This study was financially supported by the Finnish Medical Foundation, Helsinki, Finland (VVV), the Sigrid Juselius Foundation, the Folkhälsan Research Foundation, the Academy of Finland, the Helsinki University Research Funds, the Swedish Research Council, the Novo Nordisk Foundation, Konung Gustaf V:s och Drottning Victorias Frimurarestiftelse, and

Stockholm County Council (OM), the American Society of Nephrology, the Children's Discovery and Innovation Institute at the David Geffen School of Medicine, and the National Institutes of Health (DK080984 and DK098627) (KWP), The Austrian Social Health Insurance Fund (OEGK) and the Austrian Workers' Compensation Board (AUVA). Helsinki University and Helsinki University Hospital through the Doctoral Programme in Clinical Research, the Orion Research Foundation, the Finnish ORL–HNS Foundation, the Päivikki and Sakari Sohlberg Foundation, the Finnish–Norwegian Medical Foundation, the Jalmari and Rauha Ahokas Foundation, the Juhani Aho Foundation (RM).

Disclosure summary: None of the authors has any conflicts of interests with the subject material of the current manuscript.

ABSTRACT

Context: Patients with osteoporosis-associated *WNT1* or *PLS3* mutations have unique bone histomorphometric features and osteocyte-specific hormone expression patterns.

Objective: To investigate the effects of *WNT1* and *PLS3* mutations on bone material properties.

Design: Transiliac bone biopsies were evaluated by quantitative backscattered electron imaging, immunohistochemistry, and bone histomorphometry.

Setting: Ambulatory patients.

Patients: Three pediatric and eight adult patients with *WNT1* or *PLS3* mutations.

Intervention: Bone mineralization density distribution and osteocyte protein expression was evaluated in 11 patients and repeated in six patients who underwent repeat biopsy after 24 months of teriparatide treatment.

Main Outcome Measure: Bone mineralization density distribution and protein expression.

Results: Children with *WNT1* or *PLS3* mutations had heterogeneous bone matrix mineralization, consistent with bone modeling during growth. Bone matrix mineralization was homogenous in adults and increased throughout the age spectrum. Teriparatide had very little effect on matrix mineralization or bone formation in patients with *WNT1* or *PLS3* mutations. However, teriparatide decreased trabecular osteocyte lacunae size and increased trabecular bone FGF23 expression.

Conclusion: The contrast between preserved bone formation with heterogeneous mineralization in children and low bone turnover with homogenous bone mineral content in adults suggests that WNT1 and PLS3 have differential effects on bone modeling and remodeling. The lack of change in matrix mineralization in response to teriparatide, despite clear changes in osteocyte lacunae size and protein expression, suggests that altered WNT1 and PLS3 expression may interfere with

coupling of osteocyte, osteoblast, and osteoclast function. Further studies are warranted to determine the mechanism of these changes.

INTRODUCTION

Bone health and integrity are maintained by the coupled actions of bone forming osteoblasts and bone resorbing osteoclasts on the surface of trabecular bone. Together, these cells preserve bone architecture and strength by assembling discrete anatomic structures termed basic multicellular units (BMUs). Increasing evidence suggests that bone formation and bone resorption are controlled by osteocytes buried within mineralized bone (1, 2) and studies of rare monogenetic diseases associated with early-onset progressive osteoporosis offer insights into the physiology of osteocyte-specific coordination of the BMU.

Defects in the *WNT1* and *PLS3* genes underlie two monogenic forms of early-onset osteoporosis, both first characterized in 2013 (OMIM # 615221; # 300910) (3-7). Affected individuals present with low bone mineral density (BMD), peripheral fractures and multiple vertebral compression fractures, particularly in the thoracic spine (3, 5-10). The exact pathways by which *WNT1* and *PLS3* mutations cause osteoporosis remain unclear but osteocytes seem to be the major source of *WNT1* in bone and *WNT1* mutations result in impaired WNT/β-catenin signaling and decreased bone formation (11-13). By contrast, PLS3 appears to play a role in osteocyte dendrite function, skeletal mechano-sensing and osteoclastogenesis, although its exact molecular mechanisms in bone remain unknown (14, 15).

By detailed evaluation of transiliac bone biopsies, we have demonstrated that individuals affected by *WNT1* or *PLS3* mutations have unique histomorphometric measures and osteocyte-specific hormone expression patterns. In addition to low bone turnover osteoporosis, patients with a heterozygous *WNT1* mutation have increased expression and secretion of FGF23, increased numbers of marrow adipocytes, and decreased osteocyte apoptosis (16, 17). Patients with a hemizygous or heterozygous *PLS3* mutation demonstrate focal areas of defective mineralization

and elevated serum levels of the WNT inhibitor Dickkopf 1 (DKK1) (16, 17). These previous data suggest that mutations in *WNT1* and *PLS3* alter bone cell biology. How these changes in protein expression and histology relate to bone material properties at the BMU level, however, remains unknown.

In its ability to stimulate osteoblastic activity to a greater extent than osteoclastic resorption, the anabolic agent teriparatide (PTH 1–34) has putative advantages over bisphosphonates in the treatment of low-turnover osteoporosis. Clinical trials have shown that teriparatide increases BMD and reduces vertebral and peripheral fractures (18). Consistent with a PTH-induced increase in bone formation, teriparatide increases the heterogeneity of bone matrix mineralization in patients with idiopathic and postmenopausal osteoporosis, as new, lowly mineralized bone packets are formed (19-22). We have previously demonstrated that the histologic response of the skeleton to teriparatide (PTH 1–34) differs in patients with *WNT1* or *PLS3* mutations from patients with other forms of low-turnover osteoporosis. Teriparatide therapy failed to increase bone formation but resulted in a consistent decrease in eroded surface in these individuals (23), in contrast to an increase in bone erosion observed in teriparatide-treated patients with post-menopausal osteoporosis (24, 25). While this suggests that the effects of teriparatide on bone cells might be altered in these genetic forms of osteoporosis, the effects of teriparatide on bone material properties have not been investigated.

In order to further elucidate the effects of *WNT1* and *PLS3* mutations on bone at the material level, we used quantitative backscattered electron imaging (qBEI) to evaluate bone mineralization density distribution (BMDD) in a cohort of pediatric and adult patients with a *WNT1* or *PLS3* mutation. Furthermore, in order to assess how these specific mutations affect bone response to PTH at the cellular level, we evaluated the effects of teriparatide therapy on osteocyte-specific

protein expression, osteocyte lacunae size and bone material properties in a subset of the adult patients.

MATERIALS AND METHODS

Patients

We have previously described two Finnish families with monogenic osteoporosis—one caused by a heterozygous missense mutation c.652T>G (p.Cys218Gly) in *WNT1* (3) and another by a hemizygous/heterozygous splice mutation c.73–24T>A in *PLS3* (6) (**Supplemental Table**). Affected family members with a genetically verified mutation in *WNT1* or *PLS3* were invited to participate in a study characterizing skeletal and extra-skeletal features of monogenic osteoporosis. Of the mutation-positive individuals in both pedigrees, 11 patients (six with *WNT1* mutation and five with *PLS3* mutation) with low BMD and/or vertebral compression fractures underwent transiliac bone biopsy after double tetracycline labeling, as previously described (23). The demographics, biochemical values, bone histomorphometric measures, and osteocyte-specific expression patterns of these individuals have been previously described (3, 6, 16). Of these 11 individuals, a subset of six adults (*WNT1* mutation patients: n=3; *PLS3* mutation patients: n=3) participated in a longitudinal, uncontrolled, experimental study on the skeletal response to teriparatide therapy. These individuals were treated with a daily subcutaneous administration of teriparatide 20 μg (Forsteo®, Eli Lilly, USA) for 24 months. Double-labeled transiliac bone biopsies were performed at baseline and repeated after 24 months of teriparatide therapy. The study was approved by the Research Ethics Committee of the Helsinki University Central Hospital, and performed according to the ethical principles defined in the Declaration of Helsinki. The study protocol was registered in ClinicalTrials.gov (ID:NCT01360424). Changes in BMD at the patient

level and changes in bone histomorphometry in biopsies in this cohort have previously been reported (23).

Quantitative backscattered electron imaging (qBEI)

In the current analysis, BMDD was assessed by qBEI on transiliac bone cores, by a method that has been previously described (22, 26). In brief, the surface of the sample block was ground and polished to obtain a parallel surface and the sample was coated with a thin carbon layer by vacuum evaporation. qBEI was performed on a digital scanning electron microscope equipped with a four-quadrant semiconductor BE detector (DSM 962, Zeiss, Oberkochen Germany). The entire cross-sectioned bone sample area was scanned with a spatial resolution of 3.6 μm/pixel, gray-level histograms were obtained and converted into weight percent calcium (weight % Ca) histograms. The following BMDD parameters were reported separately for the trabecular and cortical compartment (arithmetic mean of both cortices, when available) of each biopsy sample: the average calcium content (CaMean, weight % Ca); the most frequently occurring calcium concentration (CaPeak, weight % Ca); the heterogeneity in mineralization (CaWidth, Δ weight % calcium) obtained as the full width at half maximum of the BMDD peak; the fraction of lowly (<17.68 weight% Ca) mineralized bone tissue (CaLow, % bone area); and the fraction of highly-mineralized (>25.30 weight % Ca) bone tissue (CaHigh, % bone area). When the biopsy sample contained the two cortices with the trabecular compartment, qBEI images were also used to assess the mineralized bone volume/tissue volume (Md BV/TV). Cortical width (Ct width all, average value from both cortices in mm), cortical porosity (Ct porosity all, average value from both cortices (%) as well as the value for each cortical plate (when available)) were also evaluated.

For evaluation of osteocyte lacunae sections (OLS), 2D image analyses were performed. The sample blocks were scanned with a Zeiss field emission scanning electron microscope (SEM SUPRA 40) with a nominal resolution of 65x (1.8 µm/pixel) and acquired qBE-images were transformed into binary images using a gray-level threshold of 5.2 weight % calcium to discriminate between unmineralized osteocyte lacunae and mineralized matrix. OLS between 5 and 200 μm^2 were extracted and analyzed with a custom-made macro in ImageJ-software (version 1.52f, Bethesda; NIH, Bethesda, MD, USA). Two parameters were evaluated separately in trabecular and cortical bone pre- and post-teriparatide (n=12): OLS-density (mean number of OLS per mineralized bone matrix area) and OLS-area (mean value in μm^2) (27).

Histomorphometric and immunohistochemical analysis of transiliac biopsies

Bone histomorphometric parameters from 6 of 11 patients of the present cohort have been previously described (3, 16, 23). Values were reported as Z-scores relative to age-matched norms (28-30). Bone protein expression from this cohort of patients at baseline has also previously been described (16); these data were now complemented with immunohistochemistry on bone biopsies obtained after 24 months of teriparatide treatment. Sections were incubated with affinity purified polyclonal goat anti-human FGF23 (225-244) (Immutopics Intl) (dilution 1:500), monoclonal anti-human DMP1 (LFMb31) (62-513) (Santa Cruz Biotechnology) (dilution 1:50), monoclonal anti-human sclerostin (MAB1406) (R&D Systems) (dilution 1:500), or polyclonal anti-human phosphor-β-catenin (ab47385) (Abcam) (dilution 1:500) primary antibodies. Immunoreactivity for FGF23 was quantified by counting the number of osteocytes expressing FGF23 in one 5 µm section of trabecular bone and normalizing this number by trabecular bone area. Immunoreactivity for DMP1, sclerostin, and phosphor-β-catenin was quantified using the Ariol SL-50 scanning

system (31) and was normalized by trabecular (for DMP1) tissue area or cortical (for sclerostin and phosphor-β-catenin) tissue area. All slides were scanned at 20 x magnification with a red filter and digitized (Applied Imaging Inc) and staining was expressed as pixels/mm^2 (31).

Statistical analysis

Measurements for normally distributed variables are reported as mean ± standard deviation (SD) and median values and interquartile range are used to describe non-normally distributed variables. Ranges are presented where noted in the text. The Wilcoxon signed rank test, Mann–Whitney U test, and the chi-squared test were used to assess inter-group differences. Relationships between mineral density, biochemical, bone histomorphometric, and immunohistochemical parameters were assessed by Spearman correlation coefficients. Changes from baseline were assessed using the paired T-test. All statistical analyses were performed using SAS software (SAS Institute Inc., Cary, NC) or GraphPad Prism, version 9.0 (GraphPad Software, San Diego, California USA) and all tests were two-sided. A probability of type I error less than 5% was considered statistically significant and ordinary p values are reported.

RESULTS

Patients

The clinical and genetic characteristics are summarized in **Supplemental Table**. Three of these patients were children (one patient with *WNT1* and two with *PLS3* mutation) and eight were adults (five with *WNT1* and three with *PLS*3 mutation). From this cohort, six adult patients (age range: 37–72 years; median age: 54 years) participated in a longitudinal study of teriparatide treatment on bone; these patients have likewise been previously characterized (23).

Bone mineralization density distribution (BMDD) in children and adults prior to teriparatide treatment.

Patients with *WNT1* and *PLS3* mutations had variable bone matrix mineralization. The one child with *WNT1* mutation had CaPeak within normal range in trabecular bone and CaMean was slightly decreased in both trabecular and cortical bone (Z-scores: -1.44 and -1.53, respectively). Concomitantly, CaLow was markedly increased (Z-scores: +2.85 and +1.95, in trabecular and cortical bone, respectively) (**Table 1, Figure 1**). This resulted in a broad heterogeneity of mineralization in both bone compartments, which is consistent with the lateral modeling drift that is observed during skeletal growth (32).

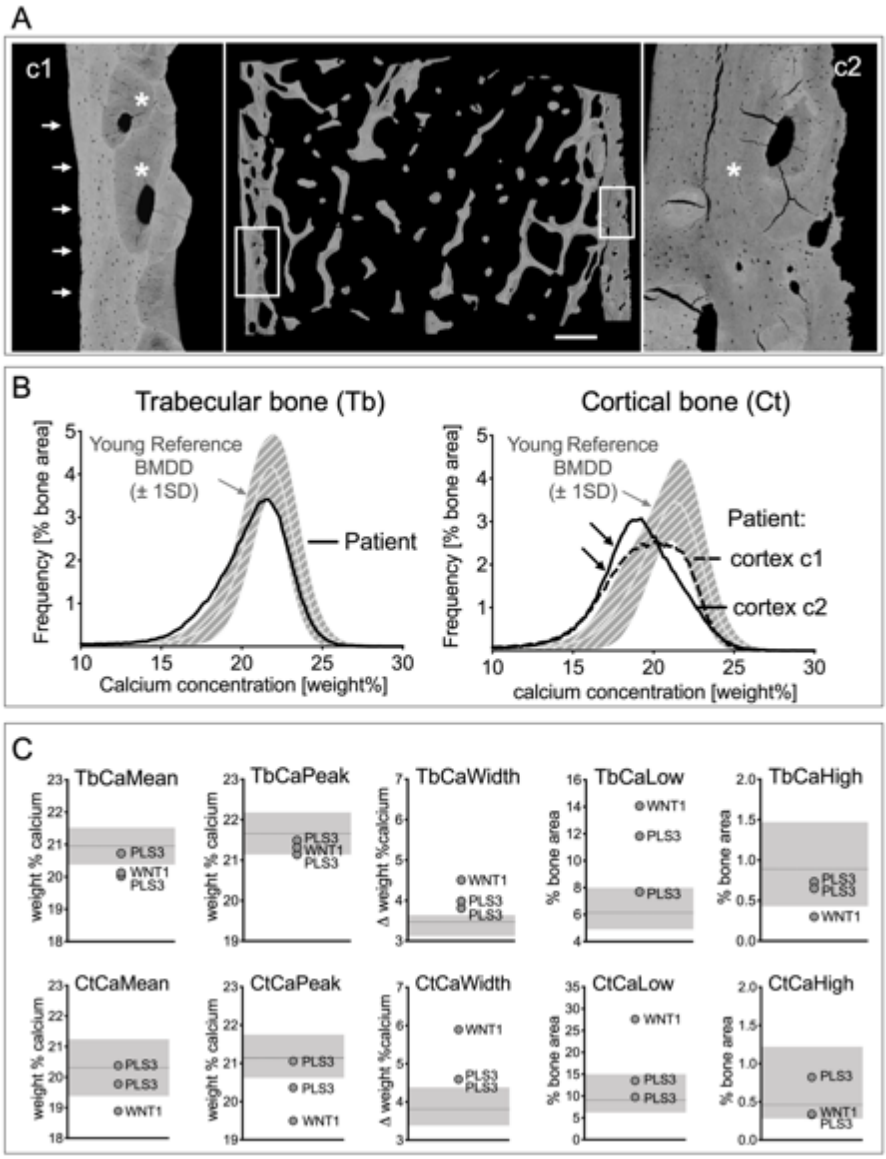

Figure 1. Backscattered electron microscopy from a transiliac bone biopsy sample of a 14-year-old male with a heterozygous *WNT1* mutation.

A. Overview of the biopsy core consisting of trabecular bone and two cortices (c1 and c2). Typical features of growth-related modeling drift are observed in the cortices (32, 33). White arrows: brighter (highly mineralized) bone matrix on the periosteal side corresponding to woven bone apposition (bone modeling) formed by the periosteum of the outer cortex. Asterisks: poorly mineralized newly formed young bone packets formed by remodeling of periosteal woven bone (c1) or compaction of drifting trabeculae (c2). The rectangles are shown magnified on the left (c1) and on the right (c2) side. Scalebar = 1mm.

B. Bone Mineralization Density Distribution (BMDD) curves for trabecular (Tb) and cortical (Ct) bone. Grey shading: reference BMDD for healthy children and adolescents (mean value ± 1SD) (32). Black arrows: slight increase in lowly mineralized bone (black arrows). The asymmetry of the cortices mirrors the increase in bone turnover typical during growth.

C. Quantitative backscattered electron imaging (qBEI) parameters results from pediatric patients with mutation in WNT1 and PLS3 are plotted for trabecular (Tb) and cortical (Ct) bone. Grey shading: normal values (mean value ± 1SD) for healthy children (32).

Table 1. Bone Mineralization Density Distribution (BMDD) parameters in children with WNT1 or PLS3 mutations.

BMDD variables	References values for children and adolescents (32)	WNT1 mutation* M, 14 yrs AIV-1	PLS3 mutation** M, 13 yrs BIV-2	PLS3 mutation** M, 9 yrs BIV-3
Trabecular bone				
CaMean (weight % Ca)	20.95 ± 0.57	**20.13**	**20.02**	20.73
CaPeak (weight % Ca)	21.66 ± 0.52	21.32	21.14	21.49
CaWidth (Δ weight % Ca)	3.47 [3.12; 3.64]	**4.51**	**3.81**	**3.99**
CaLow (% bone area)	6.14 [4.90; 7.99]	**14.07**	**11.83**	7.70
CaHigh (% bone area)	0.89 [0.43; 1.47]	0.65	**0.30**	0.73
Cortical bone				
CaMean (weight % Ca)	20.31 ± 0.93	**18.89**	19.77	20.38
CaPeak (weight % Ca)	21.14 [20.62; 21.75]	**19.50**	20.36	21.06
CaWidth (Δ weight % Ca)	3.81 [3.38; 4.38]	**5.89**	**4.59**	**4.59**
CaLow (% bone area)	9.06 [6.22; 15.00]	**27.61**	13.53	9.77
CaHigh (% bone area)	0.46 [0.28; 1.22]	0.34	0.33	0.82

TPTD=teriparatide; M=male; F=female; yrs=years. Pedigree codes are given by capital letter, Roman numeral, number. *=heterozygous WNT1 mutation p.Cys218Gly. **=hemizygous PLS3 mutation c.73–24T>A. Reference values for children are given as mean ±SD or median [interquartile range], as appropriated (32). Values deviating from normal range are in **bold**.

Trabecular BMDD parameters in adult *WNT1* patients did not differ substantially from adult reference values. CaMean Z-scores were -2.05 to +2.08; CaPeak Z-scores were -1.72 to +2.28; CaWidth Z-scores were -1.20 to +1.8; CaLow was -2.66 to -0.14; and CaHigh was -1.07 to +2.52 (**Figure 2, Table 2**).

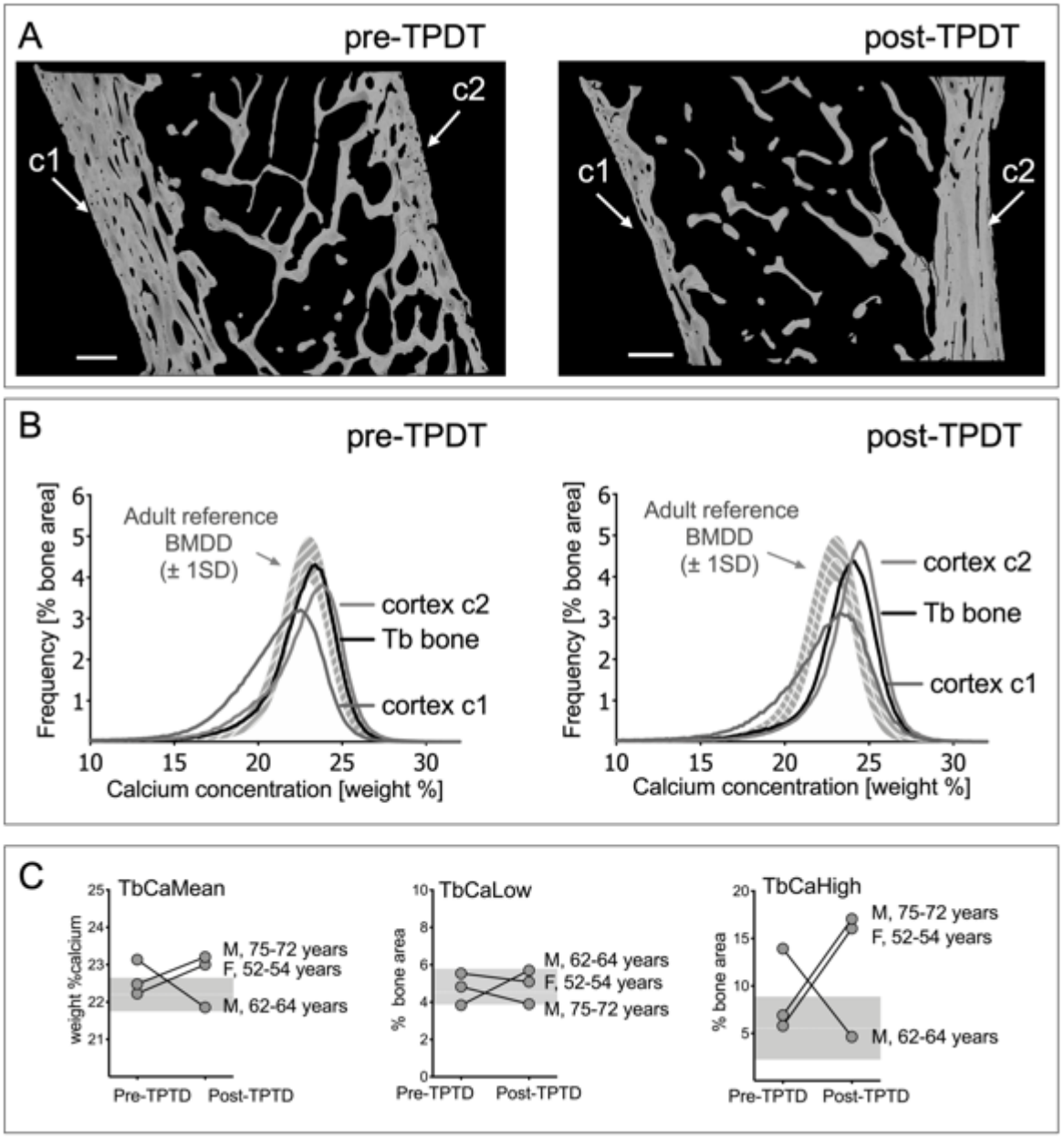

Figure 2. Backscattered electron microscopy of transiliac biopsy samples from an adult patient with a *WNT1* mutation before and after teriparatide (TPDT) treatment.
A. Overview of the biopsy core consisting of trabecular bone and two cortices (c1 and c2). The designations of c1 and c2 are arbitrarily chosen and do not designate the internal or external cortex. Scalebar =1 mm.
B. Bone Mineralization Density Distribution (BMDD) curves for trabecular (Tb) and cortical (Ct) bone. Grey shading: reference BMDD for adults (mean value ± 1SD) (22). Both cortices (c1, c2) show a marked difference in mineral content with one cortical plate being higher mineralized than the other one.
C. qBEI results in trabecular bone before and after TPDT treatment for adult patients with mutations in *WNT1*. The gray band shows the reference range (mean value ± 1SD) for adults.

Table 2. BMDD parameters in adults with a heterozygous *WNT1* missense mutation.

BMDD variables	References values for adults (22)	Pre TPTD F44 yrs AIII-2	Pre TPTD M51 yrs AIII-1	Pre TPTD F52 yrs AIII-3	Post TPTD F54 yrs AIII-3	Pre TPTD M62 yrs AII-1	Post TPTD M64 yrs AII-1	Pre TPTD M75 yrs AII-2	Post TPTD M77 yrs AII-2#
Trabecular bone									
CaMean (weight % Ca)	22.20±0.45	21.28	21.95	22.22	**23.00**	**23.14**	21.85	22.48	**23.21**
CaPeak (weight % Ca)	22.94 ±0.39	**22.18**	22.88	23.22	**23.92**	**23.92**	22.70	**23.40**	**23.92**
CaWidth (Δ weight % Ca)	3.29 [3.12; 3.47]	**3.81**	**3.99**	**3.64**	3.47	3.12	**3.64**	**2.95**	3.12
CaLow (% bone area)	4.52 [3.87; 5.79]	**6.35**	5.54	5.54	5.09	3.84	5.71	4.83	3.89
CaHigh (% bone area)	4.62 [3.52; 6.48]	**1.99**	5.80	5.80	**16.05**	**13.92**	4.63	**6.90**	**17.06**
Cortical bone									
CaMean (weight % Ca)	n.a	21.43	22.91	21.65	22.83	23.22	21.80	22.44	22.70
CaPeak (weight % Ca)	n.a	22.27	23.57	22.96	23.74	23.83	22.53	23.40	23.57
CaWidth (Δ weight % Ca)	n.a	3.81	3.47	4.42	3.90	3.47	3.81	3.73	3.99
CaLow (% bone area)	n.a	6.27	3.36	8.24	5.38	3.39	4.98	4.87	4.55
CaHigh (% bone area)	n.a	2.50	11.92	5.61	16.34	16.38	3.28	8.25	12.28

TPTD=teriparatide; M=male; F=female; yrs=years; #=only one cortex available. Pedigree codes are given by capital letter, Roman numeral, number. BMDD reference values for adults are given as mean ±SD or median [interquartile range], as appropriated (22). Of note: adult reference values for cortical bone are not available (n.a.). Values deviating from normal range are in **bold**.

CaMean, CaPeak, and CaHigh were normal or low and CaWidth was elevated in the trabecular and cortical bone of the two pediatric patients with *PLS3* mutation (**Figure 1C, Table 1**). CaLow was markedly elevated in trabecular bone of one patient (Z-score: +1.96); however, trabecular CaLow was normal in the other patient and normal in the cortical bone of both children. Adult *PLS3* patients (n=3) showed normal to slightly elevated trabecular CaMean, CaPeak, CaLow, CaHigh (Z-scores: -1.06 to +1.79; -0.61 to +1.6; -2.3 to +0.23; and -0.32 to +2.10, respectively)

while CaWidth was more variable (Z-scores: -1.12 to +2.7) (**Figure 3, Table 3**). Overall, trabecular BMDD parameters did not differ between adult patients with *WNT1* and *PLS3* mutations and no differences were observed in any trabecular BMDD parameter when compared to reference standards (22, 32). Adult reference values for cortical bone are not available for comparison; however, in paired analysis, BMDD parameters for cortical bone did not differ from those observed in trabecular bone.

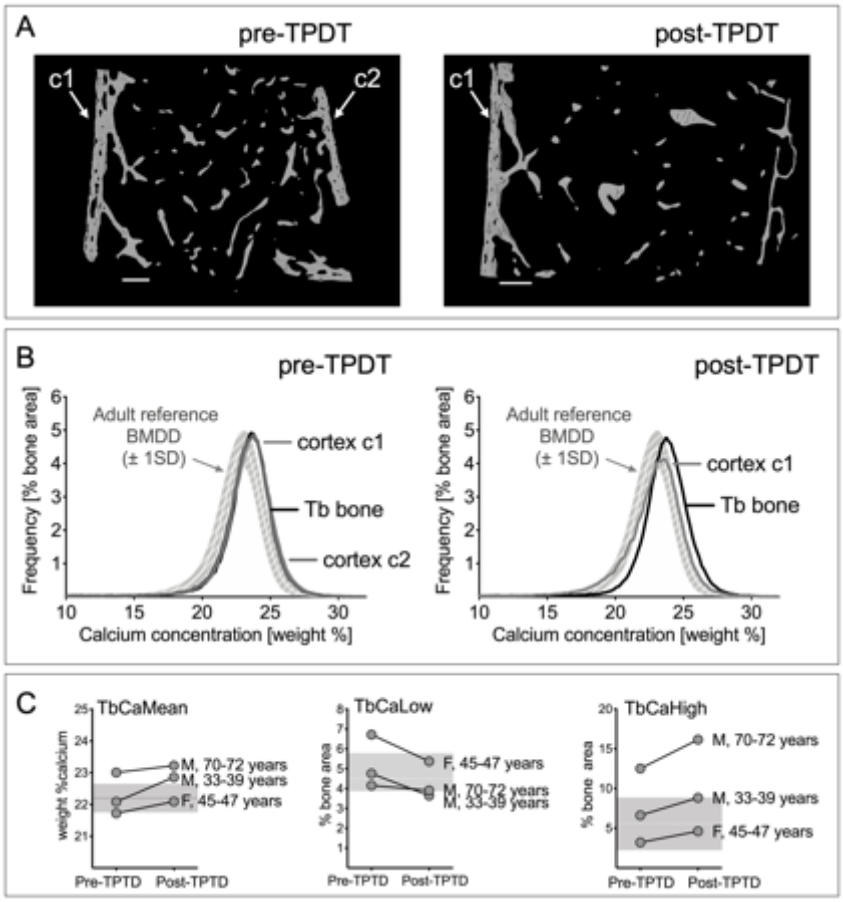

Figure 3. Backscattered electron microscopy of transiliac biopsy samples from an adult patient with a *PLS3* mutation before and after teriparatide (TPDT) treatment.
A. Representative backscattered electron microscopy images. Note that the designations of c1 and c2 are arbitrarily chosen and do not designate the internal or external cortex. Scalebar=1 mm.
B. Corresponding BMDD curves for trabecular bone (Tb) and each cortical plate (c1 and c2, respectively with one cortex only rudimentarily available after TPTD treatment). Grey shading: reference BMDD for adults (mean value ± 1SD) (22).
C. qBEI results in trabecular bone before and after TPDT treatment for adult patients with mutations in *PLS3*. The gray band shows the reference range (mean value ± 1SD) for adults.

Table 3. BMDD parameters in adults with a hemizygous/heterozygous PLS3 mutation.

BMDD variables	Reference values for adults (22)	Pre TPTD M 33yrs BIV-1	Post TPTD M 39yrs* BIV-1	Pre TPTD F45 yrs BIII-1	Post TPTD F47 yrs BIII-1	Pre TPTD M70 yrs BII-1	Post TPTD M72 yrs# BII-1
Trabecular bone							
CaMean (weight % Ca)	22.20 ± 0.45	22.22	**22.86**	**21.72**	22.09	**23.01**	**23.22**
CaPeak (weight % Ca)	22.94 ± 0.39	23.22	**23.40**	22.88	23.05	**23.57**	**23.74**
CaWidth (Δ weight % Ca)	3.29 [3.12; 3.47]	**3.64**	**2.77**	3.47	3.12	**2.95**	3.29
CaLow (% bone area)	4.52 [3.87; 5.79]	5.54	**3.64**	**6.72**	5.37	4.16	3.90
CaHigh (% bone area)	4.62 [3.52; 6.48]	5.80	8.84	3.21	4.62	12.51	16.16
Cortical bone							
CaMean (weight % Ca)	n.a	21.64	21.82	22.41	22.24	23.02	22.49
CaPeak (weight % Ca)	n.a	22.27	22.36	23.40	22.96	23.57	23.40
CaWidth (Δ weight % Ca)	n.a	4.25	3.81	3.55	3.81	3.29	3.64
CaLow (% bone area)	n.a	5.60	4.97	5.34	4.53	3.15	4.88
CaHigh (% bone area)	n.a	4.18	4.92	9.21	6.60	11.14	9.22

TPTD=teriparatide; M=male; F=female; yrs=years; #=only one cortex available; *=biopsy was obtained six years after initiating treatment. Pedigree codes are given by capital letter, roman numeral, number. BMDD reference values for adults are given as mean ± SD or median [interquartile range], as appropriated (22). Of note: adult reference values for cortical bone are not available (n.a.). Values deviating from normal range are in **bold**.

Bone mineralization density distribution and osteocyte lacunae size and density after teriparatide treatment

In adult *WNT1* and *PLS3* patients, the degree of bone matrix mineralization did not change in response to teriparatide. Paired t-test analyses showed no significant alteration in CaMean, CaPeak, CaWidth, CaLow, or CaHigh in either trabecular or cortical compartments with treatment.

A trend towards increased CaHigh was noted in trabecular (+37.6%) bone after teriparatide treatment; however, due to inter-individual variation, this change did not reach statistical significance (p=0.21). MdBV/TV ranged from 10.2% to 23.4% (mean 17.1%) pre-teriparatide treatment and 6.5% to 19.5% (mean: 14.3%) post-treatment but again, due to inter-individual variation, this change did not reach statistical significance (p=0.22). Trabecular and cortical osteocyte lacunae density and mean trabecular osteocyte lacunae area decreased significantly with teriparatide therapy while mean cortical osteocyte lacunae area did not change during teriparatide therapy (**Figure 4**).

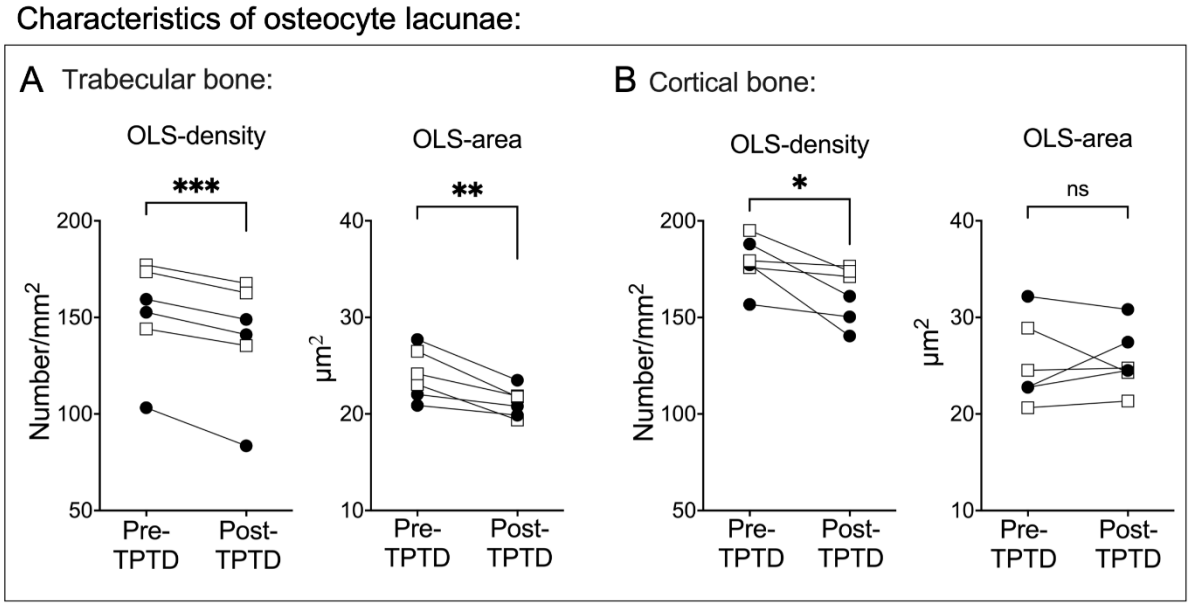

Figure 4: Change in osteocyte lacunae section (OLS) density and area in trabecular and cortical bone. Pre-TPTD: before teriparatide; Post-TPTD: after teriparatide. The asterisks indicate significant change from baseline (single: $p<0.05$; double: $p<0.01$; triple: $p<0.001$).

Relationship between BMDD parameters and patient age

When all teriparatide naïve patients were considered together (n=11, age range: 9–75 years), strong positive correlations were observed between the degree of bone matrix mineralization and patient age. These correlations were observed in both trabecular (CaMean: r=0.90, p=0.0002;

CaPeak: r=0.93, p<0.0001; CaHigh: r=0.79, p=0.0037) and cortical bone (CaMean: r=0.87, p=0.0004; CaPeak: r=0.89, p=0.0002; CaHigh: r=0.80, p=0.0032). Consistently, CaWidth, and CaLow decreased with age in trabecular (r= -0.82, p=0.0020 and r= -0.78, p=0.0045, respectively) and in cortical bone (r= -0.77, p=0.0057 and r= -0.69, p=0.0187, respectively) (**Figure 5**). Osteocyte lacunae density and area did not show any significant change with age in either cortical or trabecular bone.

Relationship between BMDD and bone histomorphometric variables and bone protein expression in baseline biopsies

We next used the previously described baseline bone histomorphometry and bone protein expression data (16) to explore their associations with baseline BMDD parameters. In the one 14-year-old patient with *WNT1* mutation, bone volume, osteoblast surface and osteoid volume were in the normal range; indeed, values for osteoid accumulation were higher in this child than in any adult with the same mutation and bone formation was squarely in the normal range. This child also had the highest numbers of FGF23 expressing osteocytes of any patient (WNT1 or PLS3) in the baseline cohort. The two children with *PLS3* mutation had lower BV/TV for age than did the cohort of *PLS3* patients as a whole; Z-scores for BV/TV were -2.9 and -1.9 in the 13-year-old and 9-year-old *PLS3* patients, respectively. As did the child with *WNT1* mutation, the two children with *PLS3* mutation had relatively preserved indices of osteoid accumulation and bone formation. This contrasted with adults in the cohort in whom osteoid accumulation and bone formation were low. Preserved histomorphometric indices of bone formation were consistent with heterogeneous matrix mineralization on qBEI. In all adult patients, osteoid surface and volume were low at

baseline and consistent with the normal to elevated bone matrix mineralization observed on qBEI in low-turnover osteoporosis.

When considering the baseline biopsies in the entire cohort, a strong negative correlation was observed between trabecular bone mineralization (CaMean) and histomorphometric variables of bone formation (OS/BS: r= -0.92, p<0.0001; ObS/BS: r= -0.95, p<0.0001; MS/BS: r= -0.91, p=0.0001; BFR/BS: r= -0.90, p=0.0001; MAR: r= -0.78, p=0.0045) but not with histomorphometric indices of bone resorption (ES/BS: r= -0.11, p=0.7497; OcS/BS r= -0.30, p=0.37). A positive correlation was observed between trabecular osteocyte lacunae area and osteoid volume (r=0.58, p=0.48). Eroded bone surface associated strongly with mineralized bone volume as measured both by histomorphometry on backscattered electron images (MdBV/TV: r=0.92, p<0.0001) and on light microscopy images (BV/TV r=0.78, p=0.0044) (**Figure 5**).

FGF23 expression was increased in patients with *WNT1* mutation as compared with those observed in normal adolescent controls. However, no correlations were observed between bone matrix mineralization and bone FGF23, DMP1, sclerostin, or β-catenin expression.

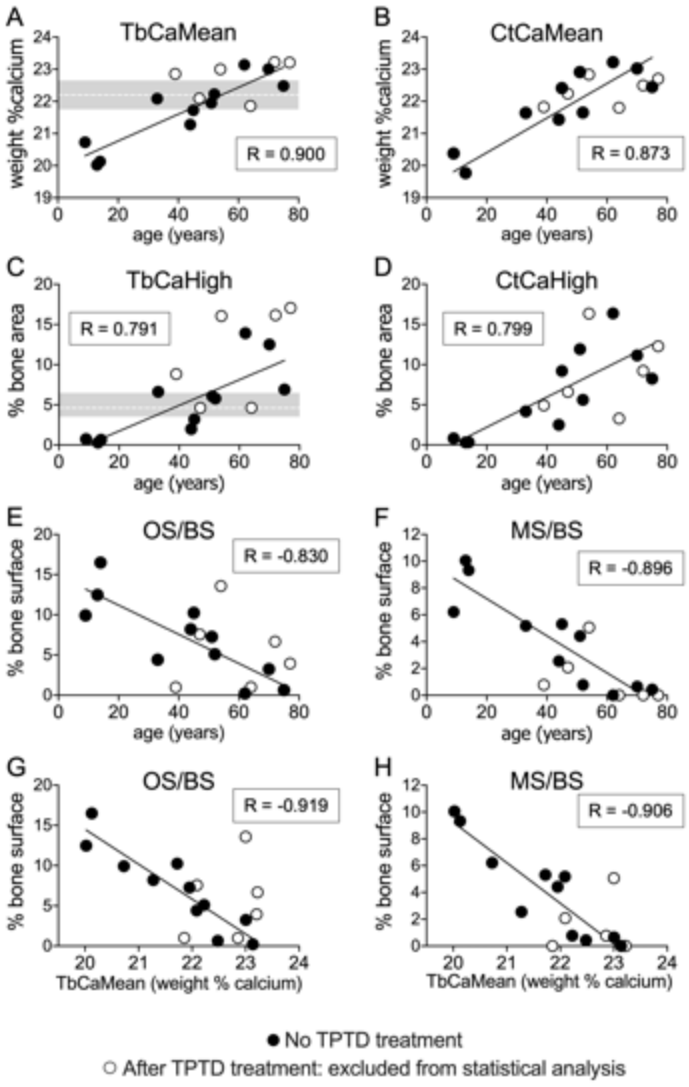

Figure 5. Association between age and the degree of bone matrix mineralization **(A, B, C, D),** age and histomorphometric indices of bone formation **(E, F)** and degree of mineralization and bone histomorphometric indices of bone formation **(G, H)**. The gray bands in **A** and **C** show the reference range for healthy adults in trabecular (Tb) bone (22). BMDD reference values for cortical (Ct) bone have not been established (**B** and **D**). The black dots represent patients who have not received teriparatide treatment (TPDT).

Relationship between BMDD, bone histomorphometry and bone protein expression after teriparatide treatment

Bone FGF23 expression increased by 126 $\pm$ 78% ($p<0.01$ from baseline) with teriparatide therapy; the magnitude of the increase in FGF23 expression did not differ based on the underlying

mutation. Teriparatide therapy increased cortical bone sclerostin expression in two out of three *PLS3* patients while leaving cortical bone sclerostin expression unchanged in all three *WNT1* patients (**Figure 6**). No consistent change in β-catenin expression was observed in either group in response to teriparatide treatment. A strong, positive, correlation was observed between eroded surface and FGF23 in the entire cohort at baseline, but not between FGF23 and measures of bone formation or osteoid accumulation. The relationship between bone matrix mineralization, variables of bone formation and age were not altered after teriparatide treatment (**Figure 5**).

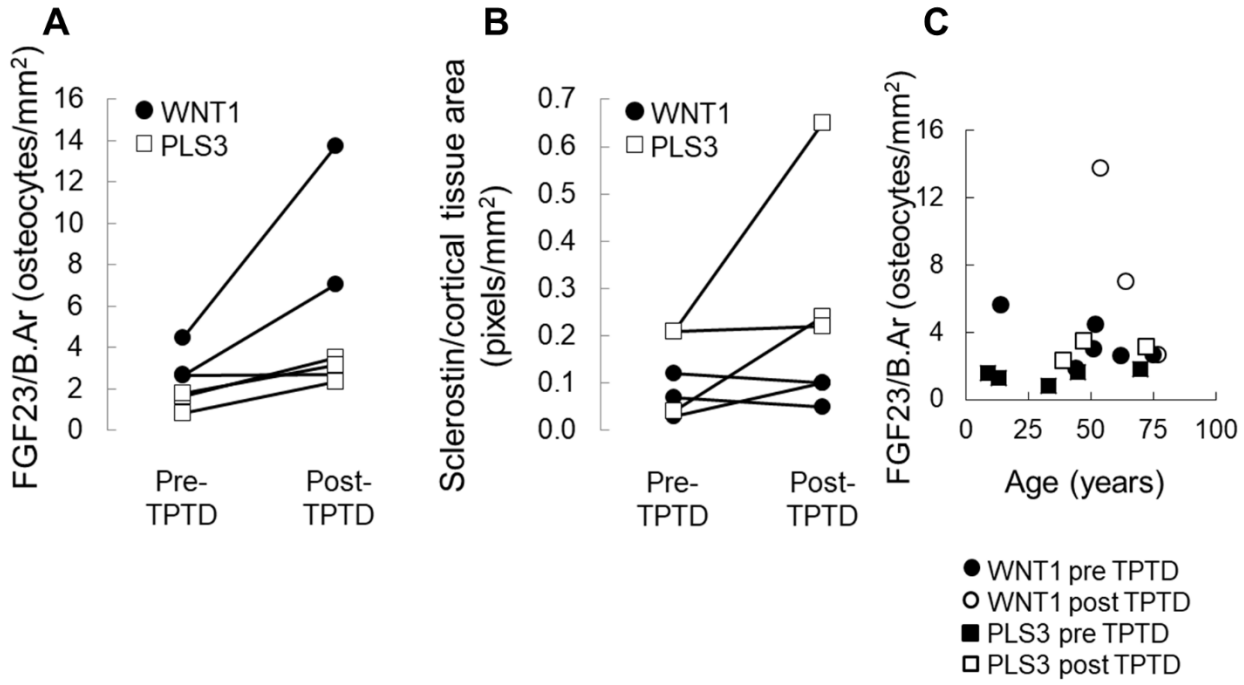

Figure 6:

A. Numbers of FGF23-expressing osteocytes in trabecular bone (FGF23/B.Ar) before and after treatment with teriparatide (TPTD) in iliac crest bone biopsies from 6 adult patients with WNT1 or PLS3 mutation. WNT1 mutation patients are depicted by closed circles; PLS3 mutation patients are depicted by open squares.
B. Sclerostin expression in cortical bone before and after treatment with teriparatide. WNT1 patients are depicted by closed circles; PLS3 patients are depicted by open squares.
C. Numbers of FGF23-expressing osteocytes in trabecular bone (FGF23/B.Ar) relative to age at time of bone biopsy. WNT1 mutation patients are depicted by circles (pre-TPTD closed; post-TPTD open); PLS3 mutation patients are depicted by squares (pre-TPTD closed; post-TPTD open).

DISCUSSION

The exact role of osteocytes in the pathogenesis of skeletal disease and the pathways by which they coordinate bone cell function and mineral accumulation at the BMU level remain incompletely defined. Our previous analyses of transiliac bone biopsy samples demonstrated that patients with *WNT1* or *PLS3* mutations have differences in osteocyte-specific protein expression and bone histomorphometry (16, 23). Here we demonstrate that these patients have normal to increased bone matrix mineralization, consistent with low-turnover osteoporosis. We also demonstrate that teriparatide, an anabolic PTH derivative, has very little effect on bone mineral content in these patients, despite altering osteocyte-specific protein expression and osteocyte lacunae size, suggesting that WNT1 and PLS3 play an important role in osteocyte-specific control of bone formation and resorption.

Mineralization is a biphasic process. Primary mineralization occurs rapidly, with 70% of final mineral content being deposited within days, while the following period of secondary mineralization, in which the remaining 30% of mineral is deposited, extends over years (34). BMDD is determined by the rate of bone turnover and the time course of mineral accumulation within the newly formed bone matrix; thus, the normal to high degree of bone matrix mineralization coupled with low bone formation rates observed in *WNT1* and *PLS3* patients is consistent with an overall decrease in bone cell activity. In low turnover osteoporosis such as this, old bone is not removed and replaced by new bone and the overall increase in tissue age leads to higher mineral content (22, 35, 36). While this kind of low-turnover osteoporosis is similar to the osteoporosis observed in elderly individuals and after glucocorticoid treatment, it contrasts with other heritable bone fragility disorders, such as Osteogenesis Imperfecta, in which bone matrix mineralization is elevated in the context of high bone remodeling, due to molecular defects in

collagen or collagen-related proteins in the extracellular matrix (37, 38). Thus, our results are in accordance with earlier observations that bone fragility in patients with *WNT1* or *PLS3* mutations is most likely related to reduced bone mass rather than low bone mass and altered bone material properties as in "brittle bone disease" (8, 9, 39-41). Despite the fact that the degree of mineralization of the matrix appears normal, permanently low bone turnover might severely impair the ability of bone to adapt to mechanical stimuli, deteriorate bone microarchitecture and lead to accumulation of micro-damage that would be otherwise removed by physiological repair processes (42, 43).

Although PTH increases bone formation—and the deposition of young bone packets with low mineral content—in other forms of low-turnover osteoporosis (19, 21, 44, 45), teriparatide did not shift the bone matrix mineralization to lower values in the majority of patients with *WNT1* and *PLS3* mutations. It is possible that an increase in bone formation did occur during the first six months of treatment and that the newly formed matrix had sufficient time to mineralize by 24 months; however, this should have led to an increase in bone mass, an increase in trabecular bone volume, and an increase in cortical width and porosity, none of which were observed. It is also noteworthy that eroded surface decreased in the trabecular compartment in these teriparatide-treated patients, in contrast to the typical increase in bone erosion observed in teriparatide-treated patients with post-menopausal osteoporosis (23). Thus, it is likely that there was very little physiological response to teriparatide, at least in iliac crest, in most of this patient cohort. A defective osteoblast response to PTH has previously been reported in some patients with idiopathic osteoporosis who have very low baseline bone formation indices (46) and it cannot be excluded that some of these "non-responders" may have underlying genetic reasons, such as mutations in *WNT1* or *PLS3*. However, although material bone properties did not change in our patients in

response to teriparatide, osteocytes did appear to sense—and respond to—the presence of PTH. Osteocyte-specific expression of FGF23 and DMP1 both increased while trabecular osteocyte lacunar size decreased during teriparatide treatment in patients with *WNT1* and *PLS3* mutations. The decrease in osteocyte lacunar size contrasts with previous reports of increased lacunar size in response to both sustained and intermittent PTH exposure paralleling an observed boost in bone formation (47-50) and suggests that osteocyte–osteoblast–osteoclast function is uncoupled in these forms of monogenic, low-turnover osteoporosis. Moreover, it is interesting to note that one male patient with *WNT1* mutation did appear to have a typical bone material response to teriparatide, with a decrease in highly mineralized bone and an increase in lowly mineralized bone. This patient had no clear differences from others in the cohort in terms of underlying genetic disease, clinical features, or prior therapies. This suggests that there are other, as yet undefined factors, that regulate bone phenotype in these patients.

Age played an important role in the observed variations in BMDD and histomorphometry. All three children demonstrated bone turnover and BMDD parameters within normal pediatric reference ranges. The mixture of highly mineralized primary bone and the lowly mineralized bone in the cortex of the one child with *WNT1* mutation mirrored the typical modeling drift in the ilium that is observed during growth (32, 33) and trabecular bone volume was preserved in this child, in line with a previous report from young children with *WNT1* mutation (39). Trabecular bone volume and cortical bone thickness were low in the two children with *PLS3* mutation; however, osteoid accumulation, bone formation, and bone material properties were normal. The few histomorphometric reports to date show large variations in bone volume, bone turnover, and bone matrix mineralization in children with *PLS3* mutation (8, 10, 51, 52). This variability contrasts with the picture of uniformly low bone turnover in adults with the same mutation, who had a

consistent increase in bone mineral density with age. Previous data suggest that deficiencies in WNT1 impair osteoclast function (53), and the increase in bone mineral density in even post-menopausal women included in the current study support this hypothesis. Differences in bone material properties between children and adults further suggest that mutations in *WNT1* and *PLS3* play different roles in bone modeling than they do in bone remodeling.

We acknowledge this study to have certain limitations, mainly concerning the limited cohort size. In addition, in three biopsies (all obtained post-teriparatide treatment), only one cortical plate was available for analysis. Since mineralization and structural indices can vary between plates (54), our practice is to calculate the arithmetic mean from the two cortices for each parameter. The lack of the second cortex in three samples could account for some variability observed in these bone compartments. Also of importance, we exclusively analyzed iliac bone samples; since bone loading plays an important role in WNT-signaling (55), osteocyte-specific protein expression could differ in other parts of the skeleton. In addition, many patients in this study had previously been treated with bisphosphonates and this may have affected response to teriparatide. However, it is important to note that a similar increase in bone matrix mineralization was observed in patients who had not previously received bisphosphonates, suggesting that prior treatment did not play a major role in the lack of teriparatide response. Overall, considering the rarity of these monogenic forms of osteoporosis, the lack of knowledge in this specific subject, and the invasive nature of obtaining a bone biopsy, we believe that our unique data offers valuable insights into human bone biology and on the effects PTH has on different signaling pathways in bone. Future studies will be needed to determine how these findings differ in other forms of osteoporosis, such as juvenile osteoporosis, senile osteoporosis, and steroid-induced osteoporosis, all of which have different underlying pathogeneses.

In conclusion, the preservation of bone formation and the heterogeneity of bone matrix mineralization in children with *WNT1* or *PLS3* mutations contrast with the low-turnover, homogenously mineralized bone in adult patients, suggesting that these two genetic defects differentially affect bone modeling and remodeling. The minimal effect of teriparatide on bone matrix mineralization, despite evident effects on osteocyte-specific hormone expression, suggests that altered expression and/or function of WNT1 and PLS3 may uncouple osteocyte signaling from osteoblast and osteoclast function (i.e. bone formation and resorption) in these forms of monogenic, low-turnover osteoporosis. Further studies are warranted to determine the precise mechanisms of these changes.

ACKNOWLEDGEMENTS

The authors thank Petra Keplinger, Sonja Lueger and Phaedra Messmer for careful sample preparations and qBEI measurements at the bone laboratory of the Ludwig Boltzmann Institute of Osteology in Vienna.

REFERENCES

1. Dallas, S. L., and Bonewald, L. F. (2010) Dynamics of the transition from osteoblast to osteocyte. *Ann N Y Acad Sci* **1192**, 437-443
2. Robling, A. G., and Bonewald, L. F. (2020) The Osteocyte: New Insights. *Annu Rev Physiol* **82**, 485-506
3. Laine, C. M., Joeng, K. S., Campeau, P. M., Kiviranta, R., Tarkkonen, K., Grover, M., Lu, J. T., Pekkinen, M., Wessman, M., Heino, T. J., Nieminen-Pihala, V., Aronen, M., Laine, T., Kroger, H., Cole, W. G., Lehesjoki, A. E., Nevarez, L., Krakow, D., Curry, C. J., Cohn, D. H., Gibbs, R. A., Lee, B. H., and Makitie, O. (2013) WNT1 mutations in early-onset osteoporosis and osteogenesis imperfecta. *N Engl J Med* **368**, 1809-1816
4. Fahiminiya, S., Majewski, J., Mort, J., Moffatt, P., Glorieux, F. H., and Rauch, F. (2013) Mutations in WNT1 are a cause of osteogenesis imperfecta. *J Med Genet* **50**, 345-348
5. van Dijk, F. S., Zillikens, M. C., Micha, D., Riessland, M., Marcelis, C. L., de Die-Smulders, C. E., Milbradt, J., Franken, A. A., Harsevoort, A. J., Lichtenbelt, K. D., Pruijs, H. E., Rubio-Gozalbo, M. E., Zwertbroek, R., Moutaouakil, Y., Egthuijsen, J., Hammerschmidt, M., Bijman, R., Semeins, C. M., Bakker, A. D., Everts, V., Klein-Nulend, J., Campos-Obando, N., Hofman, A., te Meerman, G. J., Verkerk, A. J., Uitterlinden, A. G., Maugeri, A., Sistermans, E. A., Waisfisz, Q., Meijers-Heijboer, H., Wirth, B., Simon, M. E., and Pals, G. (2013) PLS3 mutations in X-linked osteoporosis with fractures. *N Engl J Med* **369**, 1529-1536
6. Laine, C. M., Wessman, M., Toiviainen-Salo, S., Kaunisto, M. A., Mayranpaa, M. K., Laine, T., Pekkinen, M., Kroger, H., Valimaki, V. V., Valimaki, M. J., Lehesjoki, A. E., and Makitie, O. (2015) A novel splice mutation in PLS3 causes X-linked early onset low-turnover osteoporosis. *J Bone Miner Res* **30**, 510-518
7. Makitie, R. E., Costantini, A., Kampe, A., Alm, J. J., and Makitie, O. (2019) New Insights Into Monogenic Causes of Osteoporosis. *Front Endocrinol (Lausanne)* **10**, 70
8. Fahiminiya, S., Majewski, J., Al-Jallad, H., Moffatt, P., Mort, J., Glorieux, F. H., Roschger, P., Klaushofer, K., and Rauch, F. (2014) Osteoporosis caused by mutations in PLS3: clinical and bone tissue characteristics. *J Bone Miner Res* **29**, 1805-1814
9. Lu, Y., Ren, X., Wang, Y., Bardai, G., Sturm, M., Dai, Y., Riess, O., Zhang, Y., Li, H., Li, T., Zhai, N., Zhang, J., Rauch, F., and Han, J. (2018) Novel WNT1 mutations in children with osteogenesis imperfecta: Clinical and functional characterization. *Bone* **114**, 144-149
10. Balasubramanian, M., Fratzl-Zelman, N., O'Sullivan, R., Bull, M., Fa Peel, N., Pollitt, R. C., Jones, R., Milne, E., Smith, K., Roschger, P., Klaushofer, K., and Bishop, N. J. (2018) Novel PLS3 variants in X-linked osteoporosis: Exploring bone material properties. *Am J Med Genet A* **176**, 1578-1586
11. Kampe, A. J., Makitie, R. E., and Makitie, O. (2015) New Genetic Forms of Childhood-Onset Primary Osteoporosis. *Horm Res Paediatr* **84**, 361-369
12. Joeng, K. S., Lee, Y. C., Lim, J., Chen, Y., Jiang, M. M., Munivez, E., Ambrose, C., and Lee, B. H. (2017) Osteocyte-specific WNT1 regulates osteoblast function during bone homeostasis. *J Clin Invest* **127**, 2678-2688
13. Luther, J., Yorgan, T. A., Rolvien, T., Ulsamer, L., Koehne, T., Liao, N., Keller, D., Vollersen, N., Teufel, S., Neven, M., Peters, S., Schweizer, M., Trumpp, A., Rosigkeit, S., Bockamp, E., Mundlos, S., Kornak, U., Oheim, R., Amling, M., Schinke, T., and

David, J. P. (2018) Wnt1 is an Lrp5-independent bone-anabolic Wnt ligand. *Sci Transl Med* **10**
14. Boudin, E., Fijalkowski, I., Hendrickx, G., and Van Hul, W. (2016) Genetic control of bone mass. *Mol Cell Endocrinol* **432**, 3-13
15. Neugebauer, J., Heilig, J., Hosseinibarkooie, S., Ross, B. C., Mendoza-Ferreira, N., Nolte, F., Peters, M., Holker, I., Hupperich, K., Tschanz, T., Grysko, V., Zaucke, F., Niehoff, A., and Wirth, B. (2018) Plastin 3 influences bone homeostasis through regulation of osteoclast activity. *Hum Mol Genet* **27**, 4249-4262
16. Wesseling-Perry, K., Makitie, R. E., Valimaki, V. V., Laine, T., Laine, C. M., Valimaki, M. J., Pereira, R. C., and Makitie, O. (2017) Osteocyte Protein Expression Is Altered in Low-Turnover Osteoporosis Caused by Mutations in WNT1 and PLS3. *J Clin Endocrinol Metab* **102**, 2340-2348
17. Makitie, R. E., Kampe, A., Costantini, A., Alm, J. J., Magnusson, P., and Makitie, O. (2020) Biomarkers in WNT1 and PLS3 Osteoporosis: Altered Concentrations of DKK1 and FGF23. *J Bone Miner Res*
18. Minisola, S., Cipriani, C., Grotta, G. D., Colangelo, L., Occhiuto, M., Biondi, P., Sonato, C., Vigna, E., Cilli, M., and Pepe, J. (2019) Update on the safety and efficacy of teriparatide in the treatment of osteoporosis. *Ther Adv Musculoskelet Dis* **11**, 1759720X19877994
19. Misof, B. M., Roschger, P., Cosman, F., Kurland, E. S., Tesch, W., Messmer, P., Dempster, D. W., Nieves, J., Shane, E., Fratzl, P., Klaushofer, K., Bilezikian, J., and Lindsay, R. (2003) Effects of intermittent parathyroid hormone administration on bone mineralization density in iliac crest biopsies from patients with osteoporosis: a paired study before and after treatment. *J Clin Endocrinol Metab* **88**, 1150-1156
20. Misof, B. M., Paschalis, E. P., Blouin, S., Fratzl-Zelman, N., Klaushofer, K., and Roschger, P. (2010) Effects of 1 year of daily teriparatide treatment on iliacal bone mineralization density distribution (BMDD) in postmenopausal osteoporotic women previously treated with alendronate or risedronate. *J Bone Miner Res* **25**, 2297-2303
21. Dempster, D. W., Cosman, F., Zhou, H., Nieves, J. W., Bostrom, M., and Lindsay, R. (2016) Effects of Daily or Cyclic Teriparatide on Bone Formation in the Iliac Crest in Women on No Prior Therapy and in Women on Alendronate. *J Bone Miner Res* **31**, 1518-1526
22. Roschger, P., Paschalis, E. P., Fratzl, P., and Klaushofer, K. (2008) Bone mineralization density distribution in health and disease. *Bone* **42**, 456-466
23. Valimaki, V. V., Makitie, O., Pereira, R., Laine, C., Wesseling-Perry, K., Maatta, J., Kirjavainen, M., Viljakainen, H., and Valimaki, M. J. (2017) Teriparatide Treatment in Patients With WNT1 or PLS3 Mutation-Related Early-Onset Osteoporosis: A Pilot Study. *J Clin Endocrinol Metab* **102**, 535-544
24. Stepan, J. J., Burr, D. B., Li, J., Ma, Y. L., Petto, H., Sipos, A., Dobnig, H., Fahrleitner-Pammer, A., Michalska, D., and Pavo, I. (2010) Histomorphometric changes by teriparatide in alendronate-pretreated women with osteoporosis. *Osteoporos Int* **21**, 2027-2036
25. Recker, R. R., Bare, S. P., Smith, S. Y., Varela, A., Miller, M. A., Morris, S. A., and Fox, J. (2009) Cancellous and cortical bone architecture and turnover at the iliac crest of postmenopausal osteoporotic women treated with parathyroid hormone 1-84. *Bone* **44**, 113-119

26. Roschger, P., Fratzl, P., Eschberger, J., and Klaushofer, K. (1998) Validation of quantitative backscattered electron imaging for the measurement of mineral density distribution in human bone biopsies. *Bone* **23**, 319-326
27. Blouin, S., Fratzl-Zelman, N., Glorieux, F. H., Roschger, P., Klaushofer, K., Marini, J. C., and Rauch, F. (2017) Hypermineralization and High Osteocyte Lacunar Density in Osteogenesis Imperfecta Type V Bone Indicate Exuberant Primary Bone Formation. *J Bone Miner Res* **32**, 1884-1892
28. Glorieux, F. H., Travers, R., Taylor, A., Bowen, J. R., Rauch, F., Norman, M., and Parfitt, A. M. (2000) Normative data for iliac bone histomorphometry in growing children. *Bone* **26**, 103-109
29. Hoikka, V., and Arnala, I. (1981) Histomorphometric normal values of the iliac crest cancellous bone in a Finnish autopsy series. *Annals of clinical research* **13**, 383-386
30. Melsen, F., and Mosekilde, L. (1978) Tetracycline double-labeling of iliac trabecular bone in 41 normal adults. *Calcified tissue research* **26**, 99-102
31. Pereira, R. C., Jüppner, H., Azucena-Serrano, C. E., Yadin, O., Salusky, I. B., and Wesseling-Perry, K. (2009) Patterns of FGF-23, DMP1, and MEPE expression in patients with chronic kidney disease. *Bone* **45**, 1161-1168
32. Fratzl-Zelman, N., Roschger, P., Misof, B. M., Pfeffer, S., Glorieux, F. H., Klaushofer, K., and Rauch, F. (2009) Normative data on mineralization density distribution in iliac bone biopsies of children, adolescents and young adults. *Bone* **44**, 1043-1048
33. Parfitt, A. M., Travers, R., Rauch, F., and Glorieux, F. H. (2000) Structural and cellular changes during bone growth in healthy children. *Bone* **27**, 487-494
34. Ruffoni, D., Fratzl, P., Roschger, P., Klaushofer, K., and Weinkamer, R. (2007) The bone mineralization density distribution as a fingerprint of the mineralization process. *Bone* **40**, 1308-1319
35. Boivin, G., and Meunier, P. J. (2002) Changes in bone remodeling rate influence the degree of mineralization of bone. *Connect Tissue Res* **43**, 535-537
36. Ruffoni, D., Fratzl, P., Roschger, P., Phipps, R., Klaushofer, K., and Weinkamer, R. (2008) Effect of temporal changes in bone turnover on the bone mineralization density distribution: a computer simulation study. *J Bone Miner Res* **23**, 1905-1914
37. Bishop, N. (2016) Bone Material Properties in Osteogenesis Imperfecta. *J Bone Miner Res* **31**, 699-708
38. Marini, J. C., Forlino, A., Bachinger, H. P., Bishop, N. J., Byers, P. H., Paepe, A., Fassier, F., Fratzl-Zelman, N., Kozloff, K. M., Krakow, D., Montpetit, K., and Semler, O. (2017) Osteogenesis imperfecta. *Nat Rev Dis Primers* **3**, 17052
39. Palomo, T., Al-Jallad, H., Moffatt, P., Glorieux, F. H., Lentle, B., Roschger, P., Klaushofer, K., and Rauch, F. (2014) Skeletal characteristics associated with homozygous and heterozygous WNT1 mutations. *Bone* **67**, 63-70
40. Canalis, E., and Delany, A. M. (2002) Mechanisms of glucocorticoid action in bone. *Ann N Y Acad Sci* **966**, 73-81
41. Currey, J. D., Brear, K., and Zioupos, P. (1996) The effects of ageing and changes in mineral content in degrading the toughness of human femora. *J Biomech* **29**, 257-260
42. Burr, D. (2003) Microdamage and bone strength. *Osteoporos Int* **14 Suppl 5**, S67-72
43. Seref-Ferlengez, Z., Kennedy, O. D., and Schaffler, M. B. (2015) Bone microdamage, remodeling and bone fragility: how much damage is too much damage? *BoneKEy reports* **4**, 644

44. Misof, B. M., Paschalis, E. P., Blouin, S., Fratzl-Zelman, N., Klaushofer, K., and Roschger, P. (2010) Effects of one year daily teriparatide treatment on iliacal bone mineralization density distribution (BMDD) in postmenopausal osteoporotic women previously treated with alendronate or risedronate. *J Bone Miner Res* **25**, 2297-303
45. Dempster, D. W., Roschger, P., Misof, B. M., Zhou, H., Paschalis, E. P., Alam, J., Ruff, V. A., Klaushofer, K., and Taylor, K. A. (2016) Differential Effects of Teriparatide and Zoledronic Acid on Bone Mineralization Density Distribution at 6 and 24 Months in the SHOTZ Study. *J Bone Miner Res* **31**, 1527-1535
46. Cohen, A., Stein, E. M., Recker, R. R., Lappe, J. M., Dempster, D. W., Zhou, H., Cremers, S., McMahon, D. J., Nickolas, T. L., Muller, R., Zwahlen, A., Young, P., Stubby, J., and Shane, E. (2013) Teriparatide for idiopathic osteoporosis in premenopausal women: a pilot study. *J Clin Endocrinol Metab* **98**, 1971-1981
47. Gardinier, J. D., Al-Omaishi, S., Rostami, N., Morris, M. D., and Kohn, D. H. (2018) Examining the influence of PTH(1-34) on tissue strength and composition. *Bone* **117**, 130-137
48. Misof, B. M., Blouin, S., Roschger, P., Werzowa, J., Klaushofer, K., and Lehmann, G. (2019) Bone matrix mineralization and osteocyte lacunae characteristics in patients with chronic kidney disease - mineral bone disorder (CKD-MBD). *J Musculoskelet Neuronal Interact* **19**, 196-206
49. Yajima, A., Inaba, M., Tominaga, Y., Nishizawa, Y., Ikeda, K., and Ito, A. (2010) Increased osteocyte death and mineralization inside bone after parathyroidectomy in patients with secondary hyperparathyroidism. *J Bone Miner Res* **25**, 2374-2381
50. Tommasini, S. M., Trinward, A., Acerbo, A. S., De Carlo, F., Miller, L. M., and Judex, S. (2012) Changes in intracortical microporosities induced by pharmaceutical treatment of osteoporosis as detected by high resolution micro-CT. *Bone* **50**, 596-604
51. Yorgan, T. A., Sari, H., Rolvien, T., Windhorst, S., Failla, A. V., Kornak, U., Oheim, R., Amling, M., and Schinke, T. (2020) Mice lacking plastin-3 display a specific defect of cortical bone acquisition. *Bone* **130**, 115062
52. Kampe, A. J., Costantini, A., Levy-Shraga, Y., Zeitlin, L., Roschger, P., Taylan, F., Lindstrand, A., Paschalis, E. P., Gamsjaeger, S., Raas-Rothschild, A., Hovel, M., Jiao, H., Klaushofer, K., Grasemann, C., and Makitie, O. (2017) PLS3 Deletions Lead to Severe Spinal Osteoporosis and Disturbed Bone Matrix Mineralization. *J Bone Miner Res* **32**, 2394-2404
53. Wang, F., Tarkkonen, K., Nieminen-Pihala, V., Nagano, K., Majidi, R. A., Puolakkainen, T., Rummukainen, P., Lehto, J., Roivainen, A., Zhang, F. P., Makitie, O., Baron, R., and Kiviranta, R. (2019) Mesenchymal Cell-Derived Juxtacrine Wnt1 Signaling Regulates Osteoblast Activity and Osteoclast Differentiation. *J Bone Miner Res* **34**, 1129-1142
54. Misof, B. M., Dempster, D. W., Zhou, H., Roschger, P., Fratzl-Zelman, N., Fratzl, P., Silverberg, S. J., Shane, E., Cohen, A., Stein, E., Nickolas, T. L., Recker, R. R., Lappe, J., Bilezikian, J. P., and Klaushofer, K. (2014) Relationship of bone mineralization density distribution (BMDD) in cortical and cancellous bone within the iliac crest of healthy premenopausal women. *Calcif Tissue Int* **95**, 332-339
55. Bonewald, L. F., and Johnson, M. L. (2008) Osteocytes, mechanosensing and Wnt signaling. *Bone* **42**, 606-615

Supplemental Table. Patient demographics and clinical data in patients with *WNT1* and *PLS3* mutations.

Pedigree Code	Sex	Age at Biopsy (years)	Gene Mutation	Peripheral Fractures (number)	Vertebral Compression Fractures	BMD T-score (Z-score*)		Prior Osteoporosis Medication
						LS	FN	
AIII-2	F	44	Heterozygous *WNT1*	4	No	-2.6	-2.0	None
AIII-1	M	51	Heterozygous *WNT1*	2	Yes	-3.0	-2.7	None
AII-2	M	75/77	Heterozygous *WNT1*	1	Yes	0.5	0.1	ZOL 2008 (3 years prior to biopsy)
BIV-3	M	9	Hemizygous *PLS3*	2	Yes	-3.1*	-1.8*	None
BIV-2	M	13	Hemizygous *PLS3*	4	Yes	-2.7*	-2.0*	None
BIV-1	M	33/39	Hemizygous *PLS3*	10	Yes	-2.7	-0.8	ZOL 2008–2011 (9 months prior to biopsy)
AII-1	M	62/64	Heterozygous *WNT1*	3	Yes	-2.70	-2.6	ZOL 2008–2010 (1 year prior to biopsy)
AIII-3	F	52/54	Heterozygous *WNT1*	0	Yes	-2.4	-1.4	RIS 2001–2003 (8 years prior to biopsy)
AIV-1	M	14	Heterozygous *WNT1*	0	Yes	-2.0*	-2.1*	None
BIII-1	F	45/47	Heterozygous *PLS3*	1	No	-2.8	-1.3	None
BII-1	M	70/72	Hemizygous *PLS3*	4	Yes	-4.0	-2.4	ALE 1992–2005 CAL 2005–2006 ZOL 2006–2008 (3 years prior to biopsy)

F=female; M=male; BMD=bone mineral density; LS=lumbar spine; FN=femoral neck; *WNT1* mutation=heterozygous missense mutation p.Cys218Gly. *PLS3* mutation=hemizygous/heterozygous mutation c.73–24T>A. RIS, risendronate; PTH, teriparatide; ZOL, zoledronic acid; PAM, pamidronate; N/A, data not available; CAL, calcitonin.